

Dust-acoustic rogue waves in an electron depleted plasma

R. K. Shikha^{a,1}, N. A. Chowdhury^{b,1}, A. Mannan^{1,2}, and A. A. Mamun^{1,3}

¹Department of Physics, Jahangirnagar University, Savar, Dhaka-1342, Bangladesh

²Institut für Mathematik, Martin Luther Universität Halle-Wittenberg, Halle, Germany

³Wazed Miah Science Research Center, Jahangirnagar University, Savar, Dhaka-1342, Bangladesh
Email: *shikha261phy@gmail.com, *nurealam1743phy@gmail.com

Abstract

A rigorous theoretical investigation is made to study the characteristics of dust-acoustic (DA) waves (DAWs) in an electron depleted unmagnetized opposite polarity dusty plasma system that contains super-thermal (κ -distributed) ions, mobile positively and negatively charged dust grains for the first time. The reductive perturbation method is employed to obtain the NLSE to explore the modulational instability (MI) conditions for DAWs as well as the formation and characteristics of gigantic rogue waves. The nonlinear and dispersion properties of the dusty plasma medium are the prime reasons behind the formation of rogue waves. The height and thickness of the DARWs associated with DAWs as well as the MI conditions of DAWs are numerically analyzed by changing different dusty plasma parameters, such as dust charges, dust and ion number densities, and ion-temperature, etc. The implications of the results for various space dusty plasma systems (viz., mesosphere, F-rings of Saturn, and cometary atmosphere, etc.) as well as laboratory dusty plasma produced by laser-matter interaction are briefly mentioned.

Keywords: NLSE, Modulational instability, Electron depletion, Rogue waves.

1. Introduction

Opposite polarity (OP) dusty plasma (OPDP) is characterised as fully ionized gas, comprising massive positively and negatively charged dust grains as well as electrons and ions, and is believed to exist in space, viz., Planetary rings [1], Jupiter's magnetosphere [2], interstellar clouds [3, 4, 5], Earth polar mesosphere [2], cometary tails [2], solar system [6, 7, 8] and laboratory situations, viz., laser-matter interaction [5]. Rao *et al.* [9] have first theoretically predicted a new kind of low-frequency dust-acoustic (DA) waves (DAWs), and this low-frequency DAWs have been further experimentally identified by Barkan *et al.* [10] in dusty plasma (DP) medium (DPM). A revolution associated with DP physics has been welcomed after experimental identification of the DAWs, and many researchers have performed various modern eigen modes, viz., DAWs [2, 3, 4], dust lattice waves [11], dust-drift waves [12], DA shock waves (DASHWs) [13], DA solitary waves (DASWs) [5] and dust-ion-acoustic waves (DIAWs) [1] in DPM to understand various nonlinear structures regarding the propagation of low frequency electrostatic perturbation.

The attachment of electrons with massive dust grains from the ambient DPM during the dust charging process is referred to as electron depletion [13, 14, 15, 16, 17, 18]. The signature of electron depletion mechanism, in which majority even sometimes all the electrons are inserted into the massive dust grains, associated to the dust can be observed in space environments, viz., F-rings of Saturn [16], Jupiter's magnetosphere [2], interstellar clouds [4], Earth polar mesosphere [2], cometary tails [2], solar system [4], and laboratory DPM. Shukla and Silin

studied DIAWs in an electron depleted DPM (EDDPM). Mamun *et al.* [14] examined solitary potentials in two components EDDPM, and found that both dust and ion densities enhance the negative potentials. Sahu and Tribeche [17] reported the small amplitude double-layers (DLs) in an unmagnetized EDDPM, and demonstrated that their model can admit both compressive and rarefactive DA DLs (DADLs) according to the properties of plasma parameters. Ferdousi *et al.* [13] studied DASHWs in two components EDDPM, and found that under consideration, their model supports both positive and negative potentials. Hossen *et al.* [2, 3] investigated DAWs in three components EDDPM having inertial massive OP dust grains (OPDGs) and inertialess non-thermal ions, and observed that the presence of the positively charged dust significantly modified the shape of DASWs and DADLs potential structures.

The super-thermal or κ -distribution [19, 20, 21, 22, 23, 24, 25, 26, 27, 28] can describe the deviation, according to the values of the super-thermal parameter κ which manifests the presence of the external force fields or wave-particle interaction, of plasma species from the thermal or Maxwellian distribution. The super-thermal or κ -distribution exchanges with the Maxwellian distribution when κ tends to infinity, i.e., $\kappa \rightarrow \infty$, and κ -distribution is normalizable for any kind of values of κ by fulfilling this condition $\kappa > 3/2$ [22, 23, 24, 26, 27, 28]. Shahmansouri and Alinejad [22] investigated DASWs in a super-thermal DPM, and found that the depth of the potential well decreases with increasing the value of κ . Kourakis and Sultana [23] examined the presence of the super-thermal particles in a DPM, and observed how the fast particles change the speed of the DIA solitons, and also found that lower κ values sup-

port faster solitons. Uddin *et al.* [24] analyzed the nonlinear propagation of positron-acoustic waves in a super-thermal plasma, and highlighted that the height of the positive potential decreases with increasing value of κ .

The modulational instability (MI), energy localization, and energy redistribution of the carrier waves are governed by the standard nonlinear Schrödinger equation (NLSE) [26, 27, 28, 29, 30, 31, 32]. Sultana and Kourakis [26] studied electron-acoustic (EA) envelope solitons in presence of super-thermal electrons, and observed that the unstable domain of EA waves increases with κ . Ahmed *et al.* [27] examined ion-acoustic waves in multi-component plasmas, and demonstrated that the critical wave number (k_c) decreases with the increase of κ . Gill *et al.* [28] investigated the MI of the DAWs in presence of super-thermal ions in a DPM, and found that the excess super-thermality of the ions enhances the stable domain of the DAWs. Saini and Kourakis [30] reported amplitude modulation of the DAWs in presence of the super-thermal ions in a DPM, and the excess super-thermality of the plasma species recognizes narrower envelope solitons. Kourakis and Shukla [32] demonstrated the MI of the DAWs in an OPDP.

Recently, Shahmansouri and Alinejad [5] demonstrated DASWs in an EDDPM in presence of super-thermal plasma species, and found that the height of the DASWs increases with the increase in the value of super-thermality of plasma particles. In this paper, we want to develop sufficient extension of previous published work [5] by presenting a real and novel three component DP model. It could be of interest to examine the MI of DAWs and formation of DA rogue waves (DARWs) by considering a three component DP model having highly charged massive OPDGs as well as inertialess ions are modelled by the super-thermal κ -distribution.

2. Model Equations

We consider a three component unmagnetized EDDPM comprising inertial negatively and positively charged massive dust grains, and κ -distributed positive ions. At equilibrium, the quasi-neutrality condition can be written as $Z_i n_{i0} + Z_+ n_{+0} \approx Z_- n_{-0}$; where n_{i0} , n_{-0} , and n_{+0} are the number densities of positive ions, negative and positive dust grains, respectively, and Z_i , Z_+ and Z_- are the charge state of the positive ion, positive and negative dust grains, respectively. So, the normalizing equations to study the DAWs are

$$\frac{\partial n_+}{\partial t} + \frac{\partial}{\partial x}(n_+ u_+) = 0, \quad (1)$$

$$\frac{\partial u_+}{\partial t} + u_+ \frac{\partial u_+}{\partial x} = -\frac{\partial \phi}{\partial x}, \quad (2)$$

$$\frac{\partial n_-}{\partial t} + \frac{\partial}{\partial x}(n_- u_-) = 0, \quad (3)$$

$$\frac{\partial u_-}{\partial t} + u_- \frac{\partial u_-}{\partial x} = s_1 \frac{\partial \phi}{\partial x}, \quad (4)$$

$$\frac{\partial^2 \phi}{\partial x^2} = s_2 n_- - (s_2 - 1)n_i - n_+, \quad (5)$$

where n_i , n_- , and n_+ are normalized by n_{i0} , n_{-0} , and n_{+0} , respectively; u_+ and u_- represent the positive and negative dust

fluid speed, respectively, normalized by the DA wave speed $C_+ = (Z_+ k_B T_i / m_+)^{1/2}$ (with T_i being temperature of ion, m_+ being positive dust mass, and k_B being the Boltzmann constant); ϕ represents the electrostatic wave potential normalized by $k_B T_i / e$ (with e being the magnitude of single electron charge); the time and space variables are, respectively, normalized by $\omega_{p_+}^{-1} = (m_+ / 4\pi e^2 Z_+^2 n_{+0})^{1/2}$, and $\lambda_{D_+} = (k_B T_i / 4\pi e^2 Z_+ n_{+0})^{1/2}$. Other parameters can be defined as $s_1 = Z_- m_+ / Z_+ m_-$ and $s_2 = Z_- n_{-0} / Z_+ n_{+0}$. It may be noted here that we have considered $m_- > m_+$, $Z_- > Z_+$, and $n_{-0} > n_{+0}$. The expression for the number density of ions following the κ -distribution [5] can be written as

$$n_i = \left[1 + \frac{\phi}{(\kappa - 3/2)} \right]^{-\kappa + \frac{1}{2}} \quad (6)$$

where the parameter κ is known as super-thermality of the ions. Now, by substituting Eq. (6) into Eq. (5), and expanding up to third order in ϕ , we obtain

$$\begin{aligned} \frac{\partial^2 \phi}{\partial x^2} + n_+ - s_2 n_- &= (1 - s_2) + M_1 \phi \\ &+ M_2 \phi^2 + M_3 \phi^3 + \dots, \end{aligned} \quad (7)$$

where

$$\begin{aligned} M_1 &= \frac{(s_2 - 1)(2\kappa - 1)}{(2\kappa - 3)}, \\ M_2 &= \frac{(1 - s_2)(2\kappa - 1)(2\kappa + 1)}{2(2\kappa - 3)^2}, \\ M_3 &= \frac{(s_2 - 1)(2\kappa - 1)(2\kappa + 1)(2\kappa + 3)}{6(2\kappa - 3)^3}. \end{aligned}$$

We note that the term on the right hand side is the contribution of positive ions.

3. Derivation of the NLSE

To study the MI of DAWs, we will derive the NLSE by employing the reductive perturbation method. So, we first introduce the stretched co-ordinates

$$\xi = \epsilon(x - v_g t), \quad (8)$$

$$\tau = \epsilon^2 t, \quad (9)$$

where v_g is the group speed and ϵ is a small parameter. Then, we can write the dependent variables as

$$n_+ = 1 + \sum_{m=1}^{\infty} \epsilon^m \sum_{l=-\infty}^{\infty} n_{+l}^{(m)}(\xi, \tau) \exp[il(kx - \omega t)], \quad (10)$$

$$u_+ = \sum_{m=1}^{\infty} \epsilon^m \sum_{l=-\infty}^{\infty} u_{+l}^{(m)}(\xi, \tau) \exp[il(kx - \omega t)], \quad (11)$$

$$n_- = 1 + \sum_{m=1}^{\infty} \epsilon^m \sum_{l=-\infty}^{\infty} n_{-l}^{(m)}(\xi, \tau) \exp[il(kx - \omega t)], \quad (12)$$

$$u_- = \sum_{m=1}^{\infty} \epsilon^m \sum_{l=-\infty}^{\infty} u_{-l}^{(m)}(\xi, \tau) \exp[il(kx - \omega t)], \quad (13)$$

$$\phi = \sum_{m=1}^{\infty} \epsilon^m \sum_{l=-\infty}^{\infty} \phi_l^{(m)}(\xi, \tau) \exp[il(kx - \omega t)]. \quad (14)$$

where k (ω) is real variables representing the carrier wave number (frequency). The derivative operators in the above equations are treated as follows:

$$\frac{\partial}{\partial t} \rightarrow \frac{\partial}{\partial t} - \epsilon v_g \frac{\partial}{\partial \xi} + \epsilon^2 \frac{\partial}{\partial \tau}, \quad (15)$$

$$\frac{\partial}{\partial x} \rightarrow \frac{\partial}{\partial x} + \epsilon \frac{\partial}{\partial \xi}. \quad (16)$$

Now, by substituting Eqs. (10)–(16) into Eqs. (1)–(4) and Eq. (7), and collecting the terms containing ϵ , the first order ($m = 1$ with $l = 1$) equations can be expressed as

$$\omega n_{+1}^{(1)} = k u_{+1}^{(1)}, \quad (17)$$

$$k \phi_1^{(1)} = \omega u_{+1}^{(1)}, \quad (18)$$

$$\omega n_{-1}^{(1)} = k u_{-1}^{(1)}, \quad (19)$$

$$k s_1 \phi_1^{(1)} = -\omega u_{-1}^{(1)}, \quad (20)$$

$$n_{+1}^{(1)} = k^2 \phi_1^{(1)} + M_1 \phi_1^{(1)} + s_2 n_{-1}^{(1)}, \quad (21)$$

these equations reduce to

$$n_{+1}^{(1)} = \frac{k^2}{\omega^2} \phi_1^{(1)}, \quad (22)$$

$$u_{+1}^{(1)} = \frac{k}{\omega} \phi_1^{(1)}, \quad (23)$$

$$n_{-1}^{(1)} = -\frac{s_1 k^2}{\omega^2} \phi_1^{(1)}, \quad (24)$$

$$u_{-1}^{(1)} = -\frac{k s_1}{\omega} \phi_1^{(1)}, \quad (25)$$

we thus obtain the dispersion relation for DAWs

$$\omega^2 = \frac{k^2(1 + s_1 s_2)}{M_1 + k^2} \quad (26)$$

The second-order ($m = 2$ with $l = 1$) equations are given by

$$n_{+1}^{(2)} = \frac{k^2}{\omega^2} \phi_1^{(2)} + \frac{2ik(v_g k - \omega)}{\omega^3} \frac{\partial \phi_1^{(1)}}{\partial \xi}, \quad (27)$$

$$u_{+1}^{(2)} = \frac{k}{\omega} \phi_1^{(2)} + \frac{i(v_g k - \omega)}{\omega^2} \frac{\partial \phi_1^{(1)}}{\partial \xi}, \quad (28)$$

$$n_{-1}^{(2)} = -\frac{s_1 k^2}{\omega^2} \phi_1^{(2)} - \frac{2iks_1(v_g k - \omega)}{\omega^3} \frac{\partial \phi_1^{(1)}}{\partial \xi}, \quad (29)$$

$$u_{-1}^{(2)} = -\frac{k s_1}{\omega} \phi_1^{(2)} - \frac{is_1(v_g k - \omega)}{\omega^2} \frac{\partial \phi_1^{(1)}}{\partial \xi}, \quad (30)$$

with compatibility condition

$$v_g = \frac{\partial \omega}{\partial k} = \frac{\omega(1 + s_1 s_2 - \omega^2)}{k(1 + s_1 s_2)}. \quad (31)$$

The coefficients of ϵ for $m = 2$ with $l = 2$ provide the second-order harmonic amplitudes which are found to be proportional to $|\phi_1^{(1)}|^2$

$$n_{+2}^{(2)} = M_4 |\phi_1^{(1)}|^2, \quad (32)$$

$$u_{+2}^{(2)} = M_5 |\phi_1^{(1)}|^2, \quad (33)$$

$$n_{-2}^{(2)} = M_6 |\phi_1^{(1)}|^2, \quad (34)$$

$$u_{-2}^{(2)} = M_7 |\phi_1^{(1)}|^2, \quad (35)$$

$$\phi_2^{(2)} = M_8 |\phi_1^{(1)}|^2, \quad (36)$$

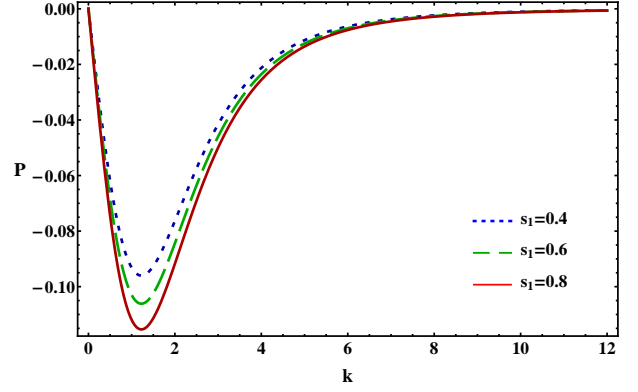


Figure 1: Plot of P vs k for various values of s_1 when $s_2 = 2.0$ and $\kappa = 1.7$.

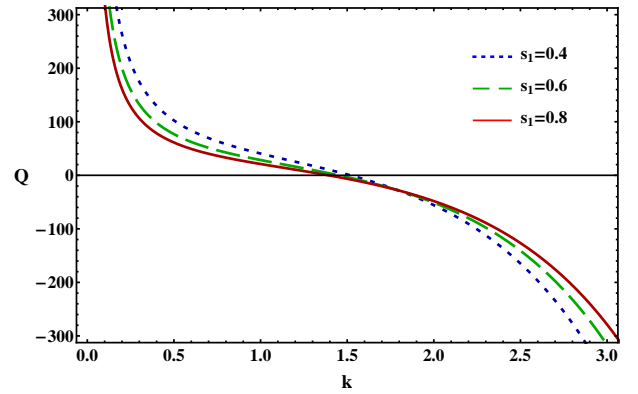


Figure 2: Plot of Q vs k for various values of s_1 when $s_2 = 2.0$ and $\kappa = 1.7$.

where

$$M_4 = \frac{3k^4 + 2M_8 \omega^2 k^2}{2\omega^4},$$

$$M_5 = \frac{k^3 + 2M_8 k \omega^2}{2\omega^3},$$

$$M_6 = \frac{3s_1^2 k^4 - 2M_8 s_1 k^2 \omega^2}{2\omega^4},$$

$$M_7 = \frac{s_1^2 k^3 - 2k s_1 M_8 \omega^2}{2\omega^3},$$

$$M_8 = \frac{2M_2 \omega^4 + 3s_2 s_1^2 k^4 - 3k^4}{2\omega^2(k^2 + s_1 s_2 k^2 - M_1 \omega^2 - 4k^2 \omega^2)}.$$

Now, we consider the expression for ($m = 3$ with $l = 0$) and ($m = 2$ with $l = 0$) which leads the zeroth harmonic modes. Thus, we obtain

$$n_{+0}^{(2)} = M_9 |\phi_1^{(1)}|^2, \quad (37)$$

$$u_{+0}^{(2)} = M_{10} |\phi_1^{(1)}|^2, \quad (38)$$

$$n_{-0}^{(2)} = M_{11} |\phi_1^{(1)}|^2, \quad (39)$$

$$u_{-0}^{(2)} = M_{12} |\phi_1^{(1)}|^2, \quad (40)$$

$$\phi_0^{(2)} = M_{13} |\phi_1^{(1)}|^2, \quad (41)$$

where

$$\begin{aligned}
M_9 &= \frac{2v_g k^3 + \omega k^2 + M_{13} v_g \omega^3}{v_g^2 \omega^3}, \\
M_{10} &= \frac{k^2 + M_{13} \omega^2}{v_g \omega^2}, \\
M_{11} &= \frac{2v_g s_1^2 k^3 + \omega k^2 s_1^2 - s_1 M_{13} \omega^3}{v_g^2 \omega^3}, \\
M_{12} &= \frac{k^2 s_1^2 - s_1 M_{13} \omega^2}{v_g \omega^2}, \\
M_{13} &= \frac{2M_2 v_g^2 \omega^3 - 2v_g k^3 - \omega k^2 + 2s_2 v_g s_1^2 k^3 + \omega s_2 k^2 s_1^2}{\omega^3 (1 + s_1 s_2 - M_1 v_g^2)}.
\end{aligned}$$

Finally, the third harmonic modes ($m = 3$) and ($l = 1$), with the help of (22)–(41), give a set of equations which can be reduced to the following NLSE:

$$i \frac{\partial \Phi}{\partial \tau} + P \frac{\partial^2 \Phi}{\partial \xi^2} + Q \Phi |\Phi|^2 = 0, \quad (42)$$

where $\Phi = \phi_1^{(1)}$ is used for simplicity. The dispersion coefficient P is

$$P = \frac{3v_g(v_g k - \omega)}{2k\omega},$$

and the nonlinear coefficient Q is

$$Q = \frac{2M_2 \omega^3 (M_8 + M_{13}) + 3M_3 \omega^3 - R}{2k^2 (1 + s_1 s_2)},$$

where

$$\begin{aligned}
R &= 2k^3 (M_5 + M_{10}) + 2s_1 s_2 k^3 (M_7 + M_{12}) \\
&\quad + \omega k^2 (M_4 + M_9) + s_1 s_2 \omega k^2 (M_6 + M_{11}).
\end{aligned}$$

It may be noted here that both P and Q are function of various plasma parameters such as k , s_1 , s_2 , and κ . So, all the plasma parameters are used to maintain the nonlinearity and the dispersion properties of the EDDPM.

4. Modulational instability and Rogue waves

The stable and unstable parametric regimes of the DAWs are organized by the sign of the dispersion (P) and nonlinear (Q) coefficients of the standard NLSE (42) [26, 27, 28, 30, 32]. When P and Q are same sign (i.e., $P/Q > 0$), the evolution of the DAWs amplitude is modulationally unstable. On the other hand, when P and Q are opposite sign (i.e., $P/Q < 0$), the DAWs are modulationally stable in presence of the external perturbations. The plot of P/Q against k yields stable and unstable domains for the DAWs. The point, at which transition of P/Q curve intersect with k -axis, is known as threshold or critical wave number k ($= k_c$).

The governing equation regarding the electron depleted DARWs in the modulationally unstable parametric regime ($P/Q > 0$) can be written as [33, 34]

$$\Phi(\xi, \tau) = \sqrt{\frac{2P}{Q}} \left[\frac{4(1 + 4iP\tau)}{1 + 16P^2\tau^2 + 4\xi^2} - 1 \right] \exp(2iP\tau). \quad (43)$$

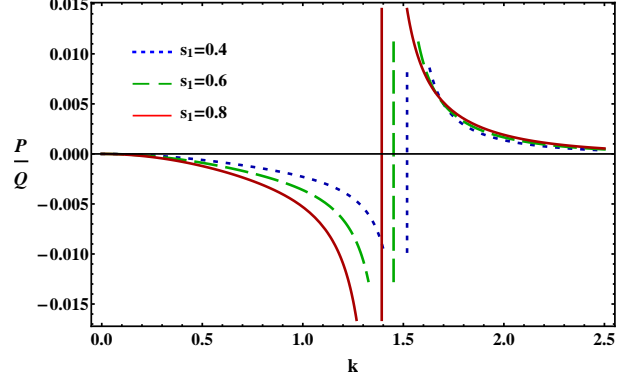


Figure 3: Plot of P/Q vs k for various values of s_1 when $s_2 = 2.0$ and $\kappa = 1.7$.

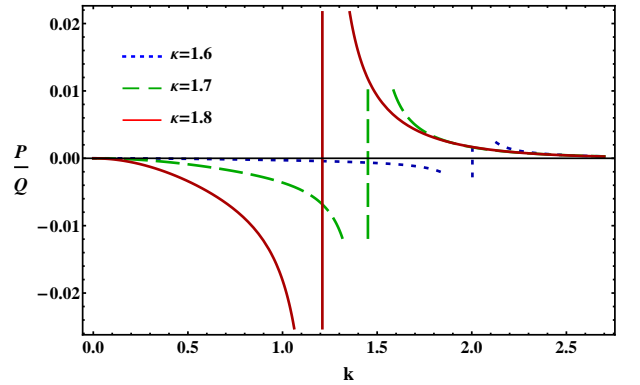


Figure 4: Plot of P/Q vs k for various values of κ when $s_1 = 0.6$ and $s_2 = 2.0$.

The plot of P/Q vs k for different plasma parameters can demonstrate the stable and unstable parametric regimes of DAWs. In the unstable parametric regime DARWs are formed in an EDDPM due to the interaction of OPDGs with ions.

5. Results and Discussion

The stability conditions of the DAWs and the formation of the DARWs can be observed from Figs. 1 to 6. It is, however, clear from Fig. 1 that (a) the P is always negative for all positive values of k ; (b) the absolute value of the P increases with increasing s_1 , i.e., charge state of the negative dust grain or mass of the positive dust grain when the charge state of the positive dust and the mass of the negative dust grains remain constant. On the other hand, from Fig. 2, it can be manifested that (a) Q is positive or negative according to the values of k and s_1 , when other plasma parameters, namely, s_2 and κ remain unchanged; (b) Q is positive (negative) for small (large) values of k . This indicates that the instability criterion of the DAWs as well as generation of the highly energetic DARWs in an EDDPM only to be determined by the sign of Q .

Figures 3 and 4 show two parametric regimes, one corresponding to the stable (i.e., $P/Q < 0$) DAWs and other corresponding to the unstable (i.e., $P/Q > 0$ and indicating the formation of the DARWs) DAWs in an EDDPM. These two parametric regimes, however, are separated by a vertical line, and

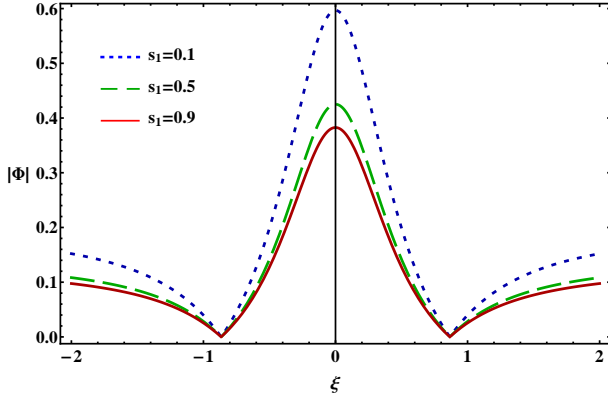


Figure 5: Plot of $|\Phi|$ vs ξ for various values of s_1 when $k = 1.6$, $\tau = 0$, $s_2 = 2.0$, and $\kappa = 1.7$.

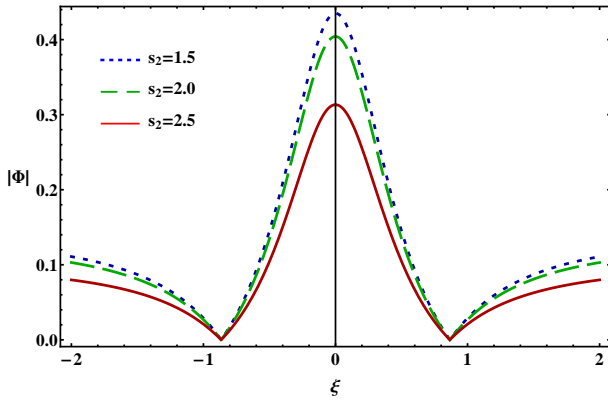


Figure 6: Plot of $|\Phi|$ vs ξ for various values of s_2 when $k = 1.6$, $\tau = 0$, $s_1 = 0.6$, and $\kappa = 1.7$.

corresponding wave number is known as critical wave number ($= k_c$) in “ P/Q versus k ” curve. The effects of positive and negative dust masses and their charge states in recognizing the stable and unstable parametric regimes associated with DAWs in an EDDPM can be observed from Fig. 3, and it is obvious from this figure that (a) the k_c decreases (increases) with an increase in the value of positive (negative) dust mass for constant value of negative and positive dust charge states; (b) on the contrary, the k_c increases (decreases) with an increase in the value of Z_+ (Z_-) for constant value of negative and positive dust masses (via s_1). So, the mass and charge state of the positive and negative dust play an opposite role in recognizing the stability of the DAWs in an EDDPM.

To examine the effects of the super-thermality of the positive ions to establish the stable and unstable parametric regimes for DAWs in an EDDPM, we have depicted Fig. 4 and this figure indicates that (a) both stable (i.e., $P/Q < 0$) and unstable (i.e., $P/Q > 0$ and indicating the formation of the DARWs) parametric regime for DAWs can exist; (b) when $\kappa = 1.6$, 1.7 , and 1.8 then the corresponding k_c value is $k_c \equiv 2.0$ (dotted blue curve), $k_c \equiv 1.5$ (dashed green curve), and $k_c \equiv 1.2$ (solid red curve); (c) so, the κ reduces the critical value hence the stable domain for the DAWs.

We have numerically analyzed Eq. (43) in Figs. 5 and 6 to understand how various plasma parameters influence the nonlinearity as well as the formation of DARWs associated with unstable parametric regime of DAWs in an EDDPM. The transformation of the amplitude of the carrier waves in a nonlinear dispersive medium is highly influenced by the existence of OPDGs and their intrinsic properties (viz., charge and mass) as they interfere with each other to organize nonlinear property, which describes the structure of the DARWs associated with DAWs in the modulationally unstable parametric regime, of the EDDPM in presence of the super-thermal ions can be seen from Figure 5, and it is clear from this figure that the nonlinearity as well as the height and thickness of the DARWs in an EDDPM having super-thermal ions increases (decreases) with increasing Z_+ (Z_-) for fixed value of m_- and m_+ (via s_1). The exact nature of the electrostatic DARWs according to the number density and charge state of the OPDGs (via s_2) can be observed from Fig. 6, and this figure exhibits that (a) the number density of negative (positive) dust in EDDPM minimizes (maximizes) the nonlinearity, i.e., the height as well as thickness of the DARWs in an EDDPM decreases (increases) in space evolution for a constant value of time as well as negative and positive dust charge states.

6. Conclusion

In this paper, we have emphasized not only the nonlinear and dispersive features of a three component EDDPM but also the stability of the DAWs and construction of DARWs by deriving a standard NLSE. The nonlinear and the dispersive coefficients of the standard NLSE reflect the stable and unstable parametric regimes of the DAWs as well as the mechanism to establish the gigantic DARWs associated DAWs in the unstable parametric regime. The numerical analysis shows that the super-thermal ions have the capability to control the MI of DAWs in an EDDPM, and also expresses that the MI conditions of the DAWs in an EDDPM are also function of the intrinsic properties (viz., charge, mass, and number density) of the massive OPDGs as well as ions. We can expect that the outcomes of our current work can be applicable in maximizing our knowledge regarding the formation of the DARWs in EDDPM which are quite connected with various space plasma, viz., the Earth polar mesosphere [2], interstellar space [3], cometary tails, Jupiter’s magnetosphere, F-rings of Saturn [16], and also laboratory plasma namely, laser-matter plasma interaction [5].

Acknowledgment

R. K. Shikha is thankful to the Bangladesh Ministry of Science and Technology for awarding the National Science and Technology (NST) Fellowship. A. Mannan gratefully acknowledges the financial support of the Alexander von Humboldt-Stiftung (Bonn, Germany).

References

- [1] P. K. Shukla and V. P. Silin, Phys. Scr. **45**, 508 (1992).

- [2] M. M. Hossen, M. S. Alam, S. Sultana, and A. A. Mamun, *Eur. Phys. J. D* **70**, 252 (2016).
- [3] M. M. Hossen, M. S. Alam, S. Sultana, and A. A. Mamun, *Phys. Plasmas* **23**, 023703 (2016).
- [4] M. M. Hossen, L. Nahar, M. S. Alam, S. Sultana, and A. A. Mamun, *High Energ. Dens. Phys.* **24**, 9 (2017).
- [5] M. Shahmansouri and H. Alinejad, *Phys. Plasmas* **20**, 033704 (2013).
- [6] M. H. Rahman, N. A. Chowdhury, A. Mannan, M. Rahman, and A. A. Mamun, *Chinese J. Phys.* **56**, 645 (2018).
- [7] N. A. Chowdhury, A. Mannan, and A. A. Mamun, *Phys. Plasmas* **24**, 113701 (2017).
- [8] S. Jahan, N. A. Chowdhury, A. Mannan, and A. A. Mamun, *Commun. Theor. Phys.* **71**, 327 (2019).
- [9] N. N. Rao, P. K. Shukla, and M. Y. Yu, *Planet. Space Sci.* **38**, 543 (1990).
- [10] A. Barkan, R. L. Merlino, and N. D. Angelo, *Phys. Plasmas* **2**, 3563 (1995).
- [11] F. Melandso, *Phys. Plasmas* **3**, 3890 (1996).
- [12] P. K. Shukla, M. Yu, and Y. R. Bharuthram, *J. Geophys. Res.* **96**, 21343 (1991).
- [13] M. Ferdousi, M. R. Miah, S. Sultana, and A. A. Mamun, *Astrophys. Space Sci.* **43**, 360 (2015).
- [14] A. A. Mamun, R. A. Cairns, and P. K. Shukla, *Phys. Plasmas* **3**, 702 (1996).
- [15] K. Dialynas, S. M. Krimigis, D. G. Mitchem, D. C. Hamilton, N. Krupp, and P. C. Brandt, *J. Geophys. Res.* **114**, A01212 (2009).
- [16] S. Mayout and M. Tribeche, *J. Plasma Phys.* **78**, 657 (2012).
- [17] B. Sahu and M. Tribeche, *Astrophys. Space Sci.* **341**, 573 (2012).
- [18] M. Ferdousi, S. Sultana, M. M. Hossen, M. R. Miah, and A. A. Mamun, *Eur. Phys. J. D* **71**, 102 (2017).
- [19] V. M. Vasyliunas, *J. Geophys. Res.* **73**, 2839 (1968).
- [20] M. H. Rahman, A. Mannan, N. A. Chowdhury, and A. A. Mamun, *Phys. Plasmas* **25**, 102118 (2018).
- [21] N. A. Chowdhury, A. Mannan, M. M. Hasan, and A. A. Mamun, *Plasma Phys. Rep.* **45**, 459 (2019).
- [22] M. Shahmansouri and H. Alinejad, *Phys. Plasmas* **19**, 123701 (2012).
- [23] I. Kourakis and S. Sultana, *AIP Conf. Proc.* **1397**, 86 (2011).
- [24] M. J. Uddin, M. S. Alam, and A. A. Mamun, *Phys. Plasmas* **22**, 062111 (2015).
- [25] N. A. Chowdhury, A. Mannan, M. R. Hossen, and A. A. Mamun, *Contrib. Plasma Phys.* **58**, 870 (2018).
- [26] S. Sultana and I. Kourakis, *Plasma Phys. Control. Fusion* **53**, 045003 (2011).
- [27] N. Ahmed, A. Mannan, N. A. Chowdhury, and A. A. Mamun, *Chaos* **28**, 123107 (2018).
- [28] T. S. Gill, A. S. Bains, and C. Bedi, *Phys. Plasmas* **17**, 013701 (2010).
- [29] N. A. Chowdhury, A. Mannan, M. M. Hasan, and A. A. Mamun, *Chaos* **27**, 093105 (2017).
- [30] N. S. Saini and I. Kourakis, *Phys. Plasmas* **15**, 123701 (2018).
- [31] N. A. Chowdhury, M. M. Hasan, A. Mannan, and A. A. Mamun, *Vacuum* **147**, 31 (2018).
- [32] I. Kourakis and P. K. Shukla, *J. Plasma Phys.* **71**, 185 (2005).
- [33] N. Akhmediev, A. Ankiewicz, and J. M. Soto-Crespo, *Phys. Rev. E* **80**, 026601 (2009).
- [34] A. Ankiewicz, N. Devine, and N. Akhmediev, *Phys. Lett. A* **373**, 3997 (2009).